

## **Design Optimization and fabrication issues of MEMS resonator**

Prasanna P. Deshpande<sup>1</sup>, Pranali M. Talekar<sup>2</sup>, Deepak G. Khushalani<sup>3</sup>, Rajesh S. Pande<sup>4</sup>

<sup>1</sup>RCOEM, Nagpur, Email: prasannapdeshpande@gmail.com

<sup>2</sup>RCOEM, Nagpur, pranali.talekar03@gmail.com

<sup>3</sup>RCOEM, Nagpur, deepak.khushalani@gmail.com

<sup>4</sup>RCOEM, Nagpur, panderaaj@yahoo.com

**Abstract**— A 1.2 GHz design optimization of microfabricated lateral field excited contour mode resonator based on MEMS (microelectromechanical system) technology for RF (radio frequency) application is presented in this paper. The emphasis is on investigating a paradigm that relieves the overly large motional resistance of the electrostatically transduced microresonators. The piezoelectric transduction provides significant advantages over capacitive transduction in terms of lower impedance, higher power handling capability and easier fabrication. The piezoelectrically transduced MEMS resonator directly replaces the off-chip filter and oscillator in the state-of-practice RF communication system and may potentially enable new wireless front-end architecture. The piezoelectric material zinc oxide is used for the better performance of the device. The geometrical parameters of the resonator determine the resonant frequency, the quality factor and the motional resistance hence the parameters need to be properly optimized. The parameter optimization ensures the best performance of the device. The optimization has been done by Taguchi method of design of experimentations followed by ANOVA (analysis of variance). The optimized dimensions have been used for simulation by COMSOL™ Multiphysics. Finally, some issues are discussed while fabricating the device.

**Keywords**— ANOVA, fabrication, LFE CM resonator, MEMS, RF, Taguchi

### **I. INTRODUCTION**

Microelectromechanical system (MEMS) is a technology that exhibits many advantages indigenous to IC technologies. Radio frequency (RF) MEMS has generated a tremendous amount of excitement because both the performance enhancements and manufacturing cost reduction are evident characteristics of the technology. At the same time as MEMS efforts continue to improve and optimize the device parameters of mechanical resonators [1]. Resonators are essential components used in RF transceivers, Bluetooth, ZigBee, wireless LAN as a filter or an oscillator. The design parameters and material of a resonator structure play an important part in MEMS technology as it impacts directly the resonant frequency, quality factor, and the motional resistance. Integrating the high-Q passives that a receiver uses onto a single chip is one path forward towards enabling the transformative reductions in size, power consumption, and cost that are desired for next-generation radios [2]. It is very important to research the progress in this area over the past years for appreciation and inspiration.

In this paper we present the design of lateral field excited contour mode resonator (LFE CM) for RF application. The device dimensions are optimized by Taguchi method optimization using analysis of variance (ANOVA). The FEM (COMSOL™ Multiphysics) based methods have been incorporated to analyse the performance parameters of microresonator before fabrication which is costly [3]. The geometrical parameters for the device design optimization of LFE CM resonator have been decided with Taguchi method of optimization. The effect of various structural parameters on the resonant frequency, motional resistance and the quality factor are studied. We were able to optimize the device parameters of the resonator to achieve our target parameters [4].

The paper is arranged as follows. The proposed design of an LFE CM microresonator device for RF application is presented using commercial CAD tool in section 2. Optimization is done for this structure using Taguchi method and the effect of change of microresonator structure on its performance parameters obtained from the Taguchi method presented in section 3. Fabrication process flow for optimized device dimensions is explained in section 4. Finally, the issues related while fabricating the device is discussed in section 5. followed by the conclusion in section 6.

## II. LFE CM MICRORESONATOR DESIGN

The MEMS resonator addressed in this paper is LFE CM which is defined with zinc oxide (ZnO) as the piezoelectric material. The zinc oxide has been chosen among all the piezoelectric material due to its better coupling coefficient; less depositing temperature, excellent bonding, environment-friendly, and its high flexibility [9]. The change in the parameters changes the resonant frequency henceforth quality factor and motional resistance. The resonant frequency  $f_0$  of the laterally vibrating mechanical structure is given by [8].

$$f_0 = (1/2wr) * \text{sqrt}(E/\rho) \quad (1)$$

Where  $wr$  is the width of sub-resonator,  $E$  is Young's modulus of elasticity and  $\rho$  is the density. Fig. 1. Shown below are the design and the simulation result using commercial CAD tool COMSOL™.

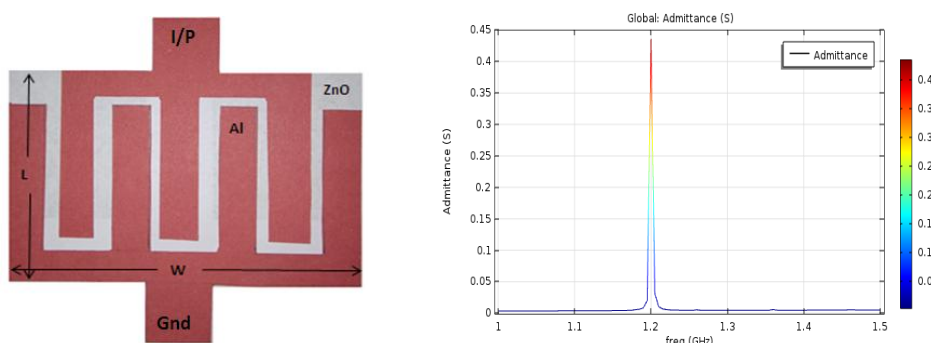


Fig. 1. (a) The design of LFE CM resonator (b) admittance vs frequency response

## III. OPTIMIZATION

For optimizing the number of parameters in our design, the numbers of combinations of control factors (input factors) have been tried. Every combination with respect to each and every control parameter is difficult to interlink and consumes a big time. So, for enhanced optimization with lesser efforts Taguchi method of design of experiments (DOE) has been implemented and then the respective analysis of variance (ANOVA) has been performed to get our vital parameters [4, 5, 6, 7]. To produce a high-quality product at low cost to the manufacturer is the basic objective of Taguchi method. It is the best suitable method where there are intermediate numbers of variables; their interactions between other variables with only a few variables are contributing significantly. Steps while performing Taguchi analysis are (i) identification of process objectives/ target parameters. In our case, these may be resonant frequency ( $f_0$ ), motional resistance ( $R_m$ ) and quality factor ( $Q$ ) (ii) finding of design parameters affecting the process. In our case these may be length, width, thickness, number of interdigitated electrodes, material used ( $E, \rho$ ) etc. (iii) creation of orthogonal array based on number of parameters and levels of variation of each parameter (iv) experimental analysis (v) ANOVA performs complete data analysis to determine the effect of the different parameters on the performance.

To optimize the design of the microresonator we have selected ten control factors which decides the important design parameters, shown in TABLE I below.

TABLE I  
 CONTROL FACTORS

Variables	Control parameters
p1	no. of sub-resonators (N)
p2	length of the resonator (L) in $\mu\text{m}$
p3	the width of top electrode ( $W_e$ ) in $\mu\text{m}$
p4	spacing/gap between two sub-resonators (s) in $\mu\text{m}$
p5	the total width of the resonator ( $N * W_r$ ) in $\mu\text{m}$
p6	the thickness of piezoelectric material (T) in $\mu\text{m}$
p7	the thickness of top metal (T top) in $\mu\text{m}$
p8	the width of sub-resonator ( $W_r$ ) in $\mu\text{m}$
p9	young's modulus of the piezoelectric material (E) in GPa
p10	the density of the piezoelectric material ( $\rho$ ) in $\text{Kg/m}^3$

Three levels are identified for each variable control factor shown in TABLE II below, considered for the analysis.

**TABLE III**  
**FACTOR LEVELS**

Factor levels	p1	p2	p3	p4	p5	p6	p7	p8	p9	p10
1	15	15	0.8	0.8	60	0.3	0.15	3	310	3260
2	21	17	1.2	0.8	60	0.2	0.1	2	112	5606
3	27	20	1	0.8	60	0.25	0.05	2.5	63	3260

The trial runs are calculated according to the L27 orthogonal array for the ten control factors with the three-factor levels to determine the resonant frequency (fo), the motional resistance (Rm) and the quality factor (Q) as target parameters shown in TABLE III below.

**TABLE IIIII**  
**EXPERIMENTAL TRIAL RUNS**

experiment	p1	p2	p3	p4	p5	p6	p7	p8	p9	p10	Rm (Ω)	fo (GHz)	Q
1	15	15	0.8	0.8	40	0.2	0.05	2	63	7600	0.013	0.72	719.79
2	15	15	0.8	0.8	50	0.25	0.1	2.5	112	5606	0.017	0.89	893.95
3	15	15	0.8	0.8	60	0.3	0.15	3	310	3260	0.020	1.63	1625.25
4	15	17	1	1	40	0.2	0.05	2.5	112	5606	0.012	0.89	893.95
5	15	17	1	1	50	0.25	0.1	3	310	3260	0.015	1.63	1625.25
6	15	17	1	1	60	0.3	0.15	2	63	7660	0.018	0.72	716.96
7	15	20	1.2	1.2	40	0.2	0.05	3	310	3260	0.010	1.63	1625.25
8	15	20	1.2	1.2	50	0.25	0.1	2	63	7660	0.013	0.72	716.96
9	15	20	1.2	1.2	60	0.3	0.15	2.5	112	5606	0.015	0.89	893.95
10	21	15	1	1.2	40	0.25	0.15	2	112	3260	0.017	1.47	1465.35
11	21	15	1	1.2	50	0.3	0.05	2.5	310	7660	0.020	1.27	1272.32
12	21	15	1	1.2	60	0.2	0.1	3	63	5606	0.013	0.56	558.72
13	21	17	1.2	0.8	40	0.25	0.15	2.5	310	7660	0.015	1.27	1272.32
14	21	17	1.2	0.8	50	0.3	0.05	3	63	3260	0.018	0.73	732.67
15	21	17	1.2	0.8	60	0.2	0.1	2	112	5606	0.012	1.12	1117.44
16	21	20	0.8	1	40	0.25	0.15	3	63	3260	0.013	0.73	732.67
17	21	20	0.8	1	50	0.3	0.05	2	112	5606	0.015	1.12	1117.44
18	21	20	0.8	1	60	0.2	0.1	2.5	310	7660	0.010	1.27	1272.32
19	27	15	1.2	1	40	0.3	0.1	2	310	5606	0.020	1.86	1859.06
20	27	15	1.2	1	50	0.2	0.15	2.5	63	3260	0.013	0.88	879.21
21	27	15	1.2	1	60	0.25	0.05	3	112	7660	0.017	0.64	637.30
22	27	17	0.8	1.2	40	0.3	0.1	2.5	63	3260	0.018	0.88	879.21
23	27	17	0.8	1.2	50	0.2	0.15	3	112	7660	0.012	0.64	637.30
24	27	17	0.8	1.2	60	0.25	0.05	2	310	5606	0.015	1.86	1859.06
25	27	20	1	0.8	40	0.3	0.1	3	112	7660	0.015	0.64	637.30
26	27	20	1	0.8	50	0.2	0.15	2	310	5606	0.010	1.86	1859.06
27	27	20	1	0.8	60	0.25	0.05	2.5	63	3260	0.013	0.88	879.21

The experimentations are statistically analysed using ANOVA to determine the percentage contribution of the individual parameters to the response [4]. The response of major contributor for respective calculations through ANOVA can be seen from Fig. 2. Below

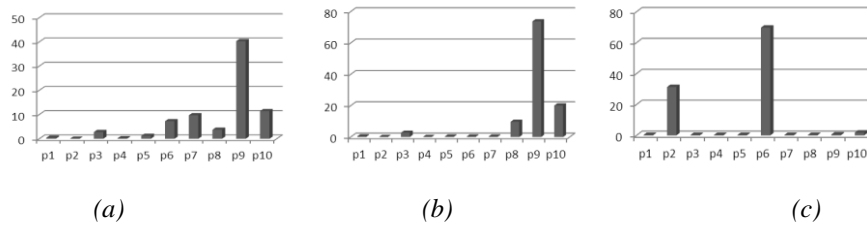


Fig. 2. Percentage contribution- (a) resonant frequency (b) quality factor (c) motional resistance

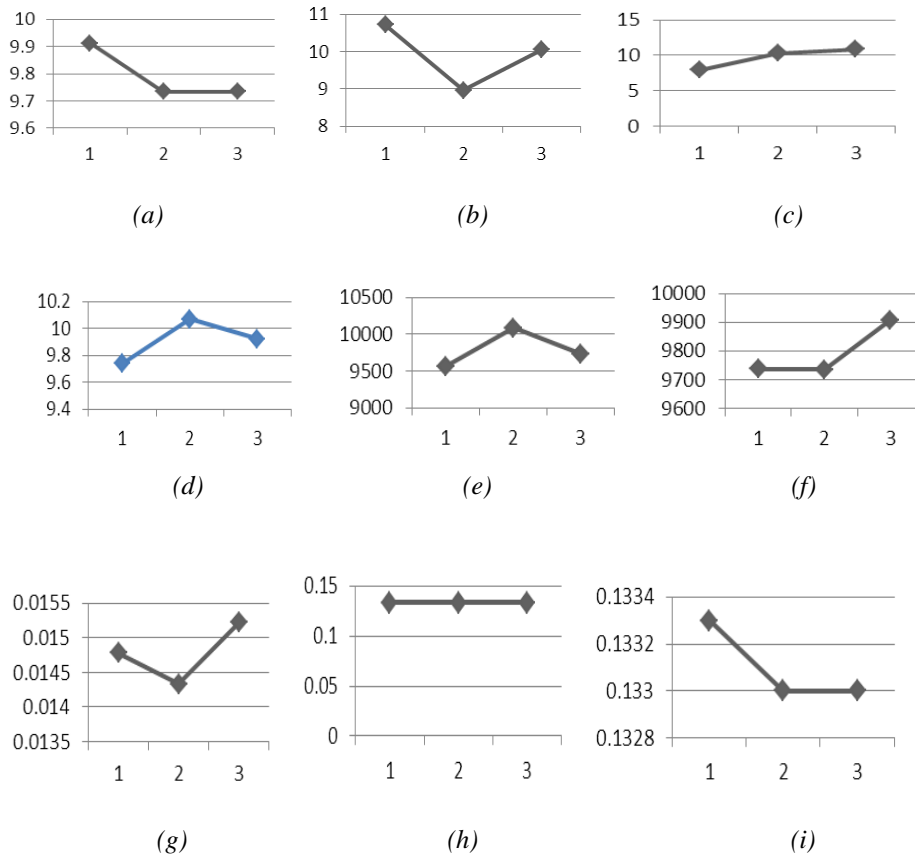


Fig. 3. Effect of – (a) length of the resonator on  $f_o$  (b) width of the resonator on  $f_o$  (c) density of the material on  $f_o$  (d) spacing between the sub resonators on  $f_o$  (e) the piezoelectric thickness on  $Q$  (f) the spacing between sub resonators on  $Q$  (g) the density of material on  $R_m$  (h) the spacing between sub resonators on  $R_m$  (i) the number of sub-resonators on  $R_m$ .

In considering the importance of the ten parameters in the design through Taguchi analysis, the best feasible design parameters have been chosen so as to match the numerical calculations. The design parameters are shown in TABLE IV below.

TABLE IV  
 EXPERIMENTAL TRIAL RUNS

Parameters	Value	Parameters	Value
Number of sub-resonators	21	Total width of Resonator	50.4 $\mu$ m
Width of top electrode	1.2 $\mu$ m	Thickness of ZnO Film	0.25 $\mu$ m
Length of Resonator	17 $\mu$ m	Thickness of top Al Film	0.1 $\mu$ m
Spacing between electrodes	1.2 $\mu$ m	Width of sub-resonator	2.4 $\mu$ m

#### IV. DEVELOPMENT OF PROCESS FLOW

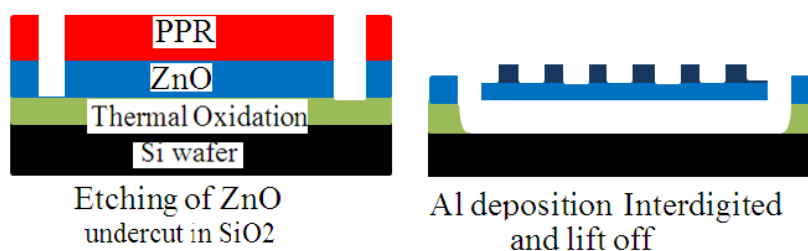


Fig. 4. Schematic of the device fabrication process flow

The process flow involves four level lithography to fabricate microresonator using surface micromachining has been developed shown in Fig. 4. A layer of silicon dioxide by wet oxidation has been deposited on a silicon wafer. The piezoelectric material ZnO was deposited on oxide layer by dielectric sputter. The first level electron beam lithography has been dedicated for alignment marks with Cr/Au liftoff. The PPR was covered for second level optical lithography for the cavity formation. The etching of ZnO has been done by phosphoric acid + acetic acid + DI water followed by silicon dioxide etching by buffered hydrofluoric acid (BHF). PMMA removal was the next step. The formation of 21 interdigitated electrodes has been done by electron beam lithography and aluminum deposition, lift off thereafter. Finally, optical lithography has been performed to deposit Cr/Au for contact pads and lifted off. The hard masks, shown in Fig. 5. have been prepared using CleWin for optical lithography process.

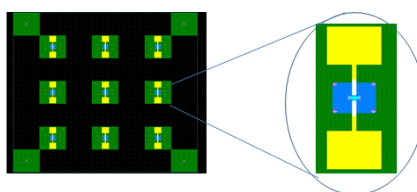


Fig. 5. Illustration of the hard mask in CleWin

#### V. FABRICATION ISSUES

While fabricating the device, the first issue faced with respect to the window openings for cavity formation in the oxide layer. The electron beam lithography on Si/SiO<sub>2</sub>/ZnO as shown in Fig. 6. (a) has been done to observe the time required to get undercut below the device. But while etching in BHF 5:1 the PMMA started peeled off within 5 minutes damaging the whole structure as shown in Fig. 6 (b) and (c).

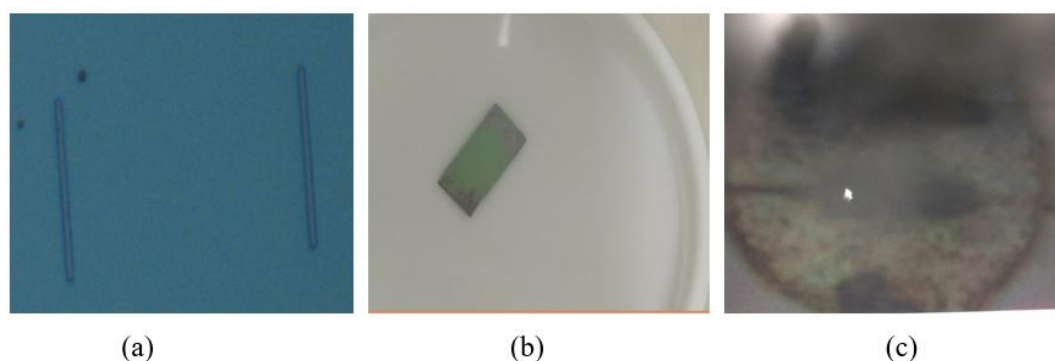


Fig. 6. (a) EBL for window opening (b) Sample in BHF PMMA started peeling (c) Structure got damaged

Some experimentation have been performed and then decided to get undercut using optical lithography as photoresist S1813 sustain in BHF. One mask plate was taken and optical lithography has been done followed by sample etched in BHF 5:1 for 18 minutes. The undercut was observed as shown in Fig.7.

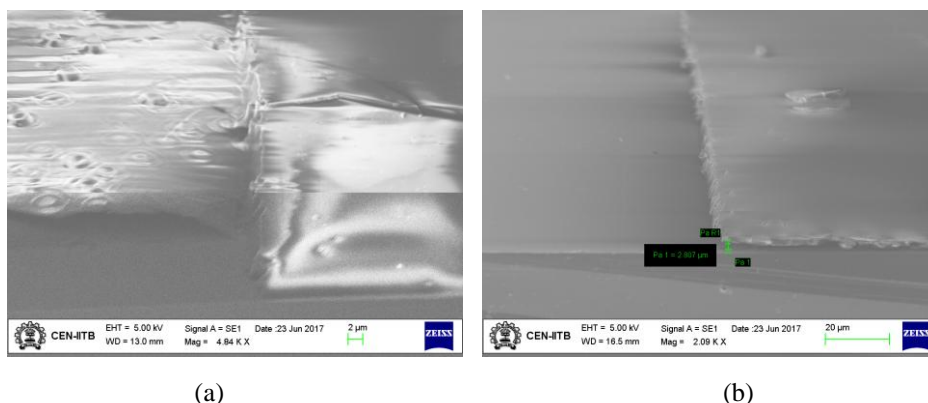


Fig. 7. Scanning electron microscope (SEM) images of (a) ZnO etch (b) undercut

The Cr/Au was deposited for alignment marks in first level electron beam lithography and put the sample for lift off for 24 hours initially but no lift-off has been processed then the sample was heated at 90 degrees for 2 hours, this results a proper lift-off.

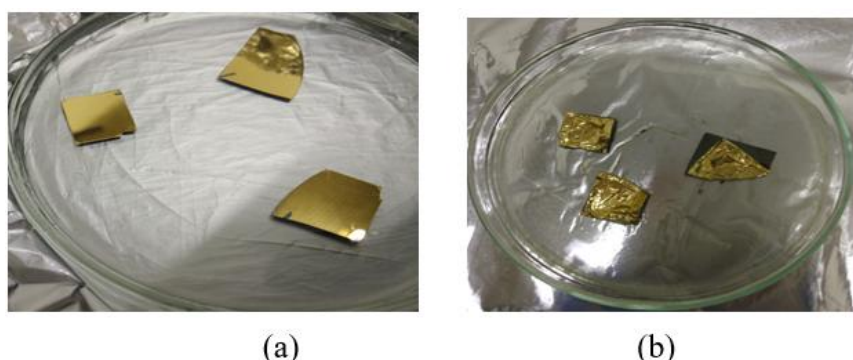
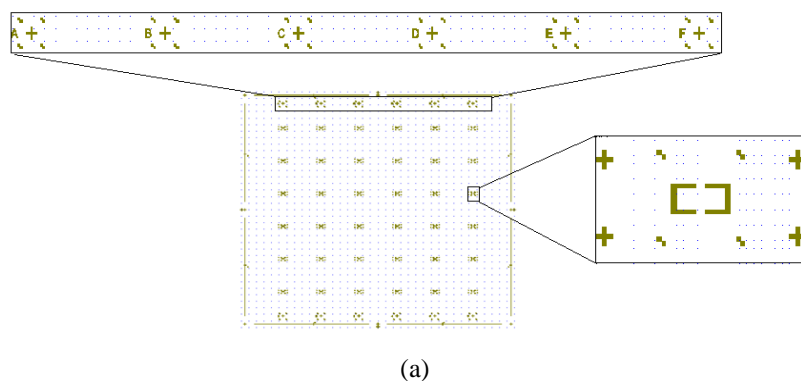


Fig. 8. (a) Image after 24-hour dip in AZ100 (no lift off observed) (b) lift off started after 1 hour of heat at 90 degree

After the lift-off, the writing of mask plate has been done for window openings by the laser writer. There are six rows and six columns shown in Fig. 9. In each column, the spacing between windows is different than that of the neighboring column because the interdigitated electrode must be accommodated between these spacing even if there is misalignment issue or reduction in spacing during BHF etch. Considering this issue, spacing was increased.



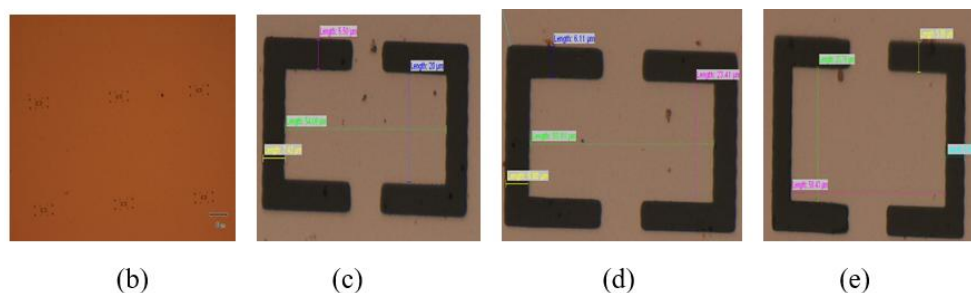


Fig. 9. (a) Mask plate in CleWin for second level lithography (b) mask plate with six devices (c) device of second column (d) device of third column (e) device of the fourth column

It was observed during second level lithography that the masks layer for electron beam lithography and optical lithography should be a mirror image of one another this is because while doing optical lithography we flip the mask plate and then UV to be exposed. The window openings were observed and the ZnO etch has been done. BHF etching for 20 minutes is also performed to get undercut (BHF 5:1 is 10nm/min) in SiO<sub>2</sub>. The Olympus microscope images are shown in Fig. 10. (a) and (b). The spacing required for interdigitated electrode was 50.4μm but it was observed that the first column was of no use as the spacing left between the windows was found less. The other columns were observed fine to use for the further process.

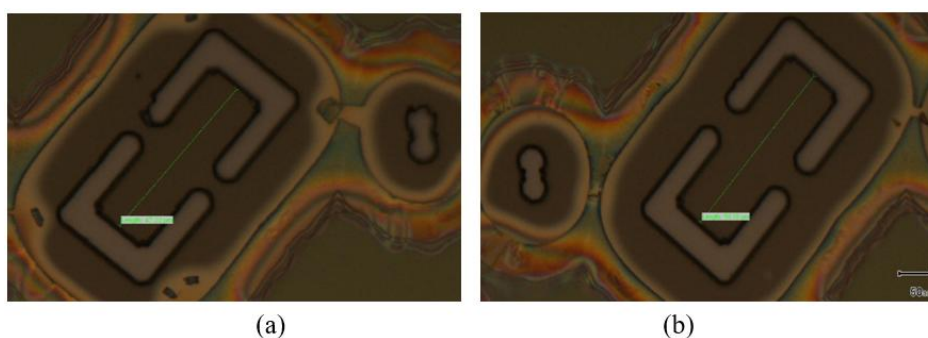


Fig. 10. (a) Window in the first column with spacing approximately 47.22μm (b) Window in the second column with spacing approximately 50.85 μm

The SEM images of these undercut as illustrated in Fig. 11(a) and (b) have been observed to check lateral etch but after etching for 20 minutes the whole pit or undercut was not obtained. So further 15 minutes etching was done and it was seen that the whole device got etched out. So, it was noted that the etching period must be between 25 to 35 minutes for a proper device.

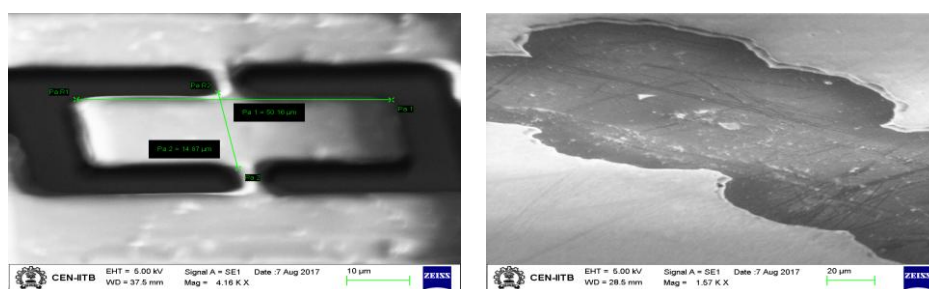


Fig. 11. (a) BHF etching for 20 minutes (b) BHF etching for 35 minutes

## VI. CONCLUSIONS

In this work the design and implementation of LFE CM resonator based on MEMS has been presented. The design parameters have been optimized by Taguchi method of design of experimentations for best feasible design. The fabrication process flow with four level lithography is also presented. The initial fabrication of the device is presented and the problem faced during fabrication was discussed, optimized and implemented in order to meet the design requirements.

## REFERENCES

- [1] J. Jason Yao, RF-MEMS from a device perspective, *J. Micromech. Microeng.*, 10(2000) R9-R38.
- [2] High-Q AlN Contour Mode Resonators with Unattached, Voltage-Actuated Electrodes, Robert Schneider, Electrical Engineering and Computer Sciences, University of California at Berkeley, Technical Report No. UCB/EECS-2015-247, December 17, 2015.
- [3] Jayu Kalambe and Rajendra Patrikar, Design, Fabrication and Characterization of Electrostatically Actuated Microcantilever Sensor for Temperature Detection, *IEEE Sensors Journal*, vol. 15, No. 3, March 2015.
- [4] Deepak G. Khushalani, Vaibhav R. Dubey, Pratik P. Bhele, Jayu P. Kalambe, Rajesh S. Pande, Rajendra M. Patrikar, Design optimization & fabrication of micro cantilever for switching application, *Sensors and Actuators A* 225 (2015)1-7
- [5] Naresh N Mahamuni, Yusuf G. Adewuyi, Application of Taguchi Method to Investigate the Effects of Process Parameters on the Transesterification of Soybean Oil Using High Frequency Ultrasound, Chemical Engineering Department North Carolina Agricultural and Technical State University Greensboro, North Carolina 27411, Energy Fuels 2010.
- [6] Il-Han Hwang, Jong-Hyun Lee, Self-actuating biosensor using a piezoelectric cantilever and its optimization, *Journal of Physics*, International MEMS Conference 2006.
- [7] Ross, P. Taguchi Techniques for Quality Engineering; McGraw-Hill: New York, 1988.
- [8] Matteo Rinaldi, Chiara Zuniga, Chengjie Zuo and Gianluca Piazza, Super-High-Frequency Two-Port AlN Contour-Mode Resonators for RF Applications, *IEEE transactions on Ultrasonics, Ferroelectrics, and Frequency control*, vol.57, No.1, January 2010
- [9] Suresh S. Balpande, Rajesh S. Pande, Rajendra M. Patrikar, Design and low cost fabrication of green vibration energy harvester, *Sensors and Actuators A: Physical*, Volume 251, 1 November 2016, Pages 134-141

## ACKNOWLEDGEMENT

The work is carried out within the framework of Indian Nanoelectronics User Program (INUP) IIT Bombay (Powai, Mumbai) India. The authors wish to acknowledge Dr. Rajendra M. Patrikar, Professor, Visvesvaraya National Institute of Technology, Nagpur (India).